PREDICTION OF TOP-DOWN CRACKING OF ASPHALT PAVEMENT LAYERS UNDER THERMAL LOADING

A Thesis

by

YU CHEN

Submitted to the Office of Graduate and Professional Studies of
Texas A&M University
in partial fulfillment of the requirements for the degree of

MASTER OF SCIENCE

Chair of Committee,	Robert L. Lytton
Committee Members,	Nasir Gharaibeh
	Rong Luo
	Anastasia Muliana
Head of Department,	Robin Autenrieth

December 2016

Major Subject: Civil Engineering

ABSTRACT

Top-down cracking is a primary fatigue cracking and widespread mode of failure in asphalt concrete pavement. Top-down cracking exists in asphalt pavement layers, initiating at the surface of the pavement and propagating downward through the asphalt layer. This phenomenon of the top-down cracking commonly occurs in the United States and has recently attracted a huge amount of interest from pavement engineers.

Top-down cracking is affected by multiple factors, including pavement materials, pavement structures, heavy traffic, and local climate. The thermal stress caused by low pavement temperature or temperature variation is a critical factor for affecting the top-down cracking in the asphalt pavement layers. The "thermal loading" is regarded as the effect of the thermal stress due to low temperature or result of temperature variation. Weather data are required for the development of the pavement temperature model and further computation of thermal stress. The climate data that contain daily air temperature, daily average wind speed, and hourly solar radiation are collected from the Long-Term Pavement Performance (LTPP) and National Climate Data Center (NCDC) databases. In addition, this pavement temperature model also requires site-specific pavement parameters, including the albedo, emissivity and absorption coefficients, and thermal conductivity for further modeling the viscoelastic thermal stress prediction. The viscoelastic thermal stress model has been developed by the finite difference solution to the viscoelastic constitutive equation based on Boltzmann's Superposition Principle using the Prony series representation of relaxation modulus. Aging of the asphalt binder is taken into account in this study.

The study develops a mechanistic-empirical approach to predict the top-down cracking under thermal loading in the asphalt pavement layer. This proposed mechanistic-empirical method is based on the modeling of pavement temperature, thermal stress, and thermal cracking. The prediction of top-down cracking in asphalt pavement layer is established by using Paris law and conducted by programming in the C# language. Its fracture coefficients are determined by pavement materials and the stress intensity factor is deduced by results from the viscoelastic thermal stress model.

DEDICATION

This thesis work is dedicated to my loving parents, Xingping Chen and Zhengping Xie for their unconditional caring, encouragement, and kind support.

ACKNOWLEDGEMENTS

Firstly, I would like to express my deepest appreciation towards my committee chair, Dr. Robert Lytton, who is my supervisor, for his continued theoretical guidance and encouragements. Special thanks to his assistance and support throughout the whole life of study at Texas A&M University. I would like to extend my gratitude to my committee members, Dr. Nasir Gharaibeh, Dr. Rong Luo, and Dr. Anastasia Muliana for their kind and great assistance and encouragements in fulfillment of my master thesis.

I would like to thank Dr. Xue Luo for her continuous and invaluable academic recommendations and help on my thesis. Many thanks go to Dr. Sheng Hu to help me C# program and Deng Yong to help me to collect climate data. Thanks also go to my friends for theirs accompany and encouragement. It has been a wonderful time with each of you at Texas A&M Univeristy.

Finally, I would like to thank my mother and father for their kindly caring, encouragement and love. Special thanks to Jin Xu who is always with me.

TABLE OF CONTENTS

LIST OF FIGURES

Page

LIST OF TABLES

Page

1. INTRODUCTION

Top-down cracking is a primary fatigue cracking and widespread mode of failure in asphalt concrete pavement. Top-down cracking exists in asphalt pavement layers initiating at the surface of the pavement and propagating downward through the asphalt layer, as shown in the figure 1. This phenomenon of the top-down cracking commonly occurs in the Unites States and has recently attracted a huge amount of interest of pavement engineers. The primary objective of this study is to develop a mechanic-empirical model for predicting top-down cracking of asphalt pavement layers under thermal loading.

Figure 1. Top-Down Cracking on US 85, Colorado [23]

Top-down cracking is affected by multiple factors including pavement materials, pavement structures, heavy traffic, and local climate. The thermal stress caused by low pavement temperature or temperature variation is a critical factor for affecting the top-down cracking in the asphalt pavement layers. The “thermal loading” is regarded as the effect of the thermal stress due to low temperature or result of temperature variation. A thermal stress response model that estimates thermal stress can be a significant part of the top-down cracking prediction. The thermal stress model was developed for predicting thermal crack length [5, 17].

The mechanisms of top-down cracking have been proposed and developed by several researchers. Some of researchers have developed experimental methods to provide material properties to assess the susceptibility of asphalt mixtures to top-down cracking [19]. Some researchers proposed hypotheses with regard to the mechanisms of top-down cracking [18]. Moreover, some researchers have conducted analytical work leading to develop the preliminary models offering the potential to estimate the initiation and propagation of top-down cracking [20]. However, these hypotheses, test method, and proposed models are limited to perform. More researches are further needed to evaluate the hypotheses and fracture models. This study is focusing on development of the thermal response model to predict the thermal-related top-down cracking.

The advantage of this study for the prediction of the thermal-related top-down cracking is using site-specific climate information, the simple mixture properties information that obtained from website database, and computer program that is needed to be developed to achieve this prediction. Required information is obtained from website database conveniently. Budget is low without the laboratory tests.

The collection of required information is crucial part of this study work. The sufficient and high-quality data are needed for this study. The weather data are required for the development of the pavement temperature model and computation of thermal stress. The climate data that contains daily average wind speed, daily air temperature, and hourly solar radiation are collected from LTPP database and NCDC database. In addition, this pavement temperature model also requires site-specific pavement parameters including the albedo, emissivity and absorption coefficients, and thermal conductivity for modeling the viscoelastic thermal stress prediction. The viscoelastic thermal stress model has been developed by the finite difference solution to the viscoelastic constitutive equation based on Boltzmann's Superposition Principle using the Prony series representation of relaxation modulus.

A mechanistic-empirical approach to predict the top-down cracking under thermal loading in the asphalt pavement layer is developed in this study. This proposed mechanistic-empirical method is primarily based on the modeling of pavement temperature, thermal stress, and fatigue cracking. The prediction of top-down cracking in asphalt pavement layer is established by using Paris law and conducted by programming in the C# language. Its fracture coefficients are determined by pavement materials and the stress intensity factor is deduced by results from the viscoelastic thermal stress model.

1.1 Research Objectives

The objective of this thesis study is intended to propose a mechanistic-empirical approach to predict the top-down cracking under thermal loading in the asphalt pavement layers with consideration of aging of asphalt binder effecting on the modulus of mixtures. The series of programs would be developed to predict the pavement temperatures, thermal stress and thermal-related top-down crack growth using the C# language and require fundamental material properties and climate data as inputs for further calculation.

1.2 Thesis Outline

This thesis is organized into five chapters. Chapter 2 provides results of literature review about the prediction of thermal-related top-down cracking in asphalt pavement layers. Chapter 3 describes in detail the modeling of thermal-related top-down cracking including the estimation of pavement temperature, thermal stress, and crack growth. Chapter 4 analyzes the results of one case study by using the proposed approach to predict the propagation of thermal-related top-down cracking and the developed computer program for entire calculations. Chapter 5 summaries the main conclusions of this study and envisions the future works.

2. LITERATURE REVIEW

This chapter provides the results of literature review about the prediction of thermal-related top-down cracking in asphalt pavement layers.

2.1 Definitions

Top-down cracking is a primary fatigue cracking and common mode of failures in asphalt concrete pavement. Top-down cracking exists in asphalt pavement layers initiating at the surface of the pavement and propagating downward through the asphalt layer.

2.2 Factors of Crack Propagation

Top-down cracking is affected by multiple factors including pavement materials, pavement structures, heavy traffic, and local climate. The results of literature reviews show that material properties as a contribution to the top-down cracking include asphalt mixture composition, modulus variation, fracture properties and thermal properties. The influence on the propagation of top-down cracking due to pavement structure includes extremely thin or thick asphalt layers and stabilized and unstablized base course. The traffic factors involve the load magnitude and distribution and load spectrum. The Climate components contain the pavement temperature, aging of asphalt binder and development of thermal stress.

2.3 Previous Research

This study focuses on thermal-related top-down cracking in asphalt pavement layers. Therefore, material properties, including asphalt mixture composition, modulus variation, fracture properties and thermal properties and climate components, including pavement temperature, aging of asphalt binder and development of thermal stress would be analyzed in this study.

The Pavement temperature was previously predicted by the Enhanced Integrated Climate Model (EICM), which is one-dimensional model with heat and moisture simulation and later incorporated into Mechanistic-Empirical Pavement Design Guide (MEPDG) to combine pavement design with modeled pavement temperature [11]. The EICM model utilizes a finite-difference approximation approach for the calculation of models of heat transfer in asphalt pavement layers involving outgoing long-wave radiation, absorption of solar radiation, convective heat transfer and a temperature boundary condition under the pavement. However, in comparison with measure pavement temperature, some large errors appeared in the prediction of pavement temperature using the EICM model [1]. The incorrect pavement temperature estimation would cause later biased calculation for the crack propagation.

A previous research conducted by Rongbin Han et al [16] proposed one applicable pavement temperature model to estimate the pavement temperature changing with depth and time. The hourly pavement temperature would be calculated by using the model-required climate data obtained from available database and optimization of site-specific pavement parameters. The model-required climate data contain daily average wind speed, hourly solar radiation, and hourly air temperature. The specific pavement parameters include albedo, emissivity, thermal diffusivity, absorption coefficient, and the model parameters, a and d. This improved pavement temperature model more accurately predict the hourly pavement temperature for a large range of pavement sections and would accepted in this study.

The National Cooperative Highway Research Project 1-41 recommends an approach to compute the viscoelastic thermal stress using general form of thermal stress integration [1]. Relaxation modulus modeled by Dirichlet series is used to calculate the viscoelastic thermals tress at the tip of crack. However, the aging of asphalt binder is not considered to effect the relaxation modulus. In this study, the finite different solution of the thermal stress integration is provided to further development of thermal stress computer program. The more coefficients of Prony series model are provided and the consideration of aging of asphalt binder is taken into this study for more accurate results of relaxation modulus.

The aging research from Luo et al. [9] targets the field pavement aging and aims at characterizing and predicting field aging using the kinetics-based modeling including the field mixture moduli and field aging temperature [9]. The calibrated parameters involving rheological activation energy and modulus activation energy are provided in this study. This kinetic-based aging prediction of asphalt mixtures is adopted in this study for calculation of aged reference modulus and aged thermal stress.

The previous studies [1,21] utilized Paris law for estimation of crack propagation in the asphalt pavement layers. Stress intensity factor is used in these research work obtained by regression equation developed by using material properties or by Artificial Neural Network model. However, the use of pseudo J-integral in this study replacing stress intensity factor would be better for the prediction of crack growth. That is because the J-integral is the way to calculate the strain energy release rate and the stress intensity factor is used to predict the stress state near the tip of crack. The J-integral could be interpreted as a plastic fracture mechanics and the stress intensity factor is used in linear elastic fracture mechanics. Moreover, the fracture parameter obtained based on material properties simplifies the estimation of crack growth without performing tests in this study.

3. MODELING OF THEORETICAL MODELS FOR TOP-DOWN CRACKING UNDER THERMAL LOADING

Chapter 3 describes in detail the modeling of thermal-related top-down cracking including the estimation of pavement temperature, thermal stress, and crack growth. The aging of asphalt binder is taken into consideration in this study for prediction of reference modulus and thermal stress.

3.1 Prediction of Temperature in an HMA Pavement Modeling

The estimation of pavement temperature is considered as the first step for predicting the thermal-related top-down cracking. Increasing the accuracy of calculating the pavement temperature with depth in a pavement structure is considered due to the relevance of the thermal stress. The pavement temperature with depth is crucial factor to accomplish the computation of thermal stress. The thermal stress is essential contribution to the growth of top-down cracking under thermal loading.

The pavement temperature model developed by the research group at Texas A&M University [1] is adopted in this study to better predict temperature variations over time and depth in asphalt pavement layers. This pavement temperature model is a new one-dimensional model developed based on energy balance between radiation and conduction energy. The heat transfer activity is presented schematically in figure 1. A variety of sources of heat transfer at the pavement surfaces are required for implementing the pavement temperature model, including solar radiation, emission by long-wave radiation to the atmosphere, absorption of atmospheric down-welling long wave radiation by pavement surface, convective heat transfer that is enhanced by wind [16]. The heat is transferred by conduction under the pavement surface and inside the pavement structure. The heat transfer enhancement by precipitation is not included in this pavement temperature model. The mathematical computation details of this pavement temperature model is described as following.

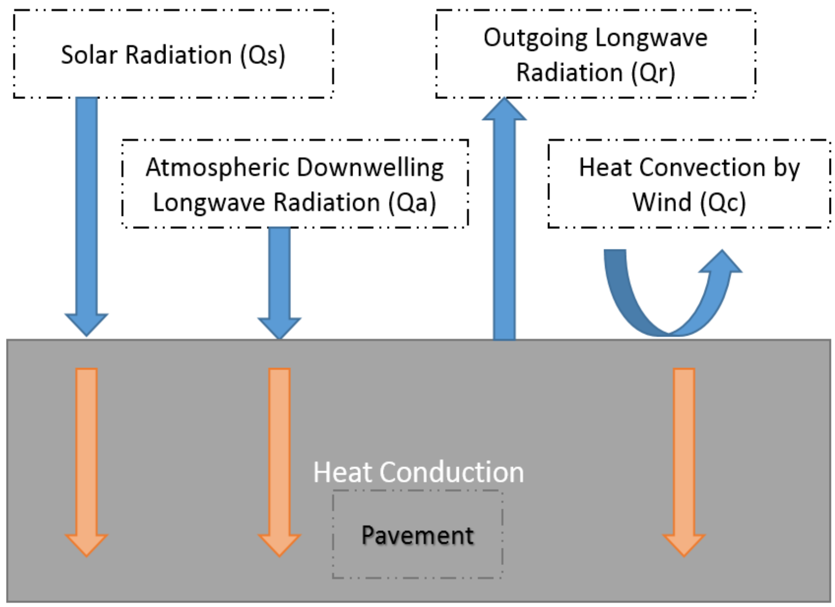

Figure 2. Graphical Representation of Heat Transfer Model of Pavement [1]

3.1.1 Heat Transfer in Pavement

The classical thermal diffusion equation provided in equation 1 is used to define heat transfer activities [16].

$$\frac{\partial T}{\partial t} = \alpha \frac{\partial^2 T}{\partial x^2} \quad (1)$$

where

T	=	the pavement temperature as a function of time and depth below pavement surface x;
α	=	the thermal diffusivity;
α	=	k/ρC where k is the thermal conductivity;
ρ	=	the density; and
C	=	the pavement heat capacity.

3.1.2 The Surface Boundary Condition

For surface boundary condition, different elements of pavement surface are considered. Because thermal energy will change to fluxes from above and inside pavement. The various fluxes presented in figure 1 contribute the following surface condition [16].

$$\rho C \frac{\Delta x}{2} \frac{\partial T_s}{\partial t} = Q_s - \tilde{\alpha} \cdot Q_s + Q_a - Q_r - Q_c - Q_f \quad (2)$$

where

ρC	=	volumetric heat capacity of the pavement;
T_s	=	pavement surface temperature;
x	=	the depth below the pavement surface;
$\frac{\Delta x}{2}$	=	the (differential) pavement thickness for the energy balance;
Q_s	=	heat flux due to solar radiation;
$\tilde{\alpha}$	=	albedo of pavement surface, the fraction of reflected solar radiation;

Q_a = down-welling long-wave radiation heat flex from the atmosphere;

Q_r = outgoing long-wave radiation heat flux from the pavement surface;

Q_c = the convective heat flex between the surface and the air; and

Q_f = the heat flux within the pavement at the pavement surface.

The absorption and emission of long-wave radiation (in $W \cdot m^{-2}$) are computed by equation 3 and 4 [16].

$$Q_a = \varepsilon_a \sigma T_a^4 \tag{3}$$

$$Q_r = \varepsilon \sigma T_s^4 \tag{4}$$

where

ϵ_a = absorption coefficient of pavements;

ϵ = emission coefficient of pavements;

T_s = pavement surface temperature, K;

T_a = air temperature, K; and

α = $5.68 \times 10^{-8} W \cdot m^{-2} K^{-4}$ is Stefan-Boltzman constant.

The convective heat flux (in $W \cdot m^{-2}$) is determined by equation 5 [16].

$$Q_c = h_c \left(T_s - T_a \right) \tag{5}$$

where

h_c = is the heat transfer coefficient from the empirical equation 6 [11].

$$h_c = 698.24 \cdot a \cdot \left[0.00144 \left(abs\left(\frac{T_s + T_a}{2} \right) \right)^{0.3} U^d + 0.0097 \left(abs\left(T_s + T_a \right) \right)^{0.3} \right] \tag{6}$$

where

U = the hourly wind speed ($i\ m \cdot s^{-1}$); and

a, d = two-dimensionless empirical parameters.

The heat flux above the pavement surface is calculated by Fourier's equation 7 [16].

$$Q_f = k \frac{\partial T_s}{\partial x} \tag{7}$$

where

T_s = pavement surface temperature; and

K = thermal conductivity of asphalt concrete (in $W \cdot m^{-1} \cdot k^{-1}$).

Combining and substituting these above equations, the thermal energy balance at the pavement surface yields the surface boundary condition, which is provided in equation 8 [16].

$$pC \frac{\Delta x}{2} \frac{\partial T_s}{\partial t} = Q_s - \tilde{\alpha} \cdot Q_s + \varepsilon_a \sigma T_a^4 - \varepsilon \sigma T_s^4 - h_c \left(T_s - T_a \right) + k \frac{\partial T_s}{\partial x} \tag{8}$$

3.1.3 The Bottom Boundary Condition

Based on literature reviews and LTPP database, it was found that the pavement temperatures beyond 2m pavement depth have a tendency in approximately linearly changing with depth. Therefore, the bottom boundary condition was utilized at a pavement depth of 3m [16].

$$\frac{\partial T_s}{\partial x}\Big|_{3m} = indenpent\ of\ \ depth \qquad (9)$$

3.1.4 Numerical Solution of Model

This pavement temperature model is implemented numerically by using a finite different approximation method. The model input data are required to solve this model, including climate data and site-specific pavement parameters. The climate data include daily average wind speed, hourly air temperature, and hourly solar radiation. The model parameters are albedo, emissivity, thermal diffusivity, absorption coefficient, and heat-transfer coefficient parameters (a and d). In this numerical solution, the pavement thickness is broke up into various cells. These cells are described as thicker close to the pavement surface and thinner downward deeper pavements and each one of these cells are specified a temperature in the beginning of the computation as an initial condition. The next step is to calculate a new temperature for each cell at each time step [16].

3.1.5 Obtaining Temperature Model Input Data and Parameters

The inputs for pavement temperature model requires precise site-specific hourly climate data and model parameters [8]. The model inputs for the climate data include as follows:

1) Hourly solar radiation;
2) Hourly air temperature; and
3) Daily average wind speed.

The other model inputs for model parameters are described in the following:

1) Albedo;

2) Emissivity;

3) Absorption coefficient;

4) Thermal diffusivity; and

5) Heat-transfer coefficient parameters (a and d).

Hourly solar radiation could be obtained from the National Solar Radiation Database (NSRDB). The Solar radiation data can be modeled by using Meteorological-Statistical (METSTAT) models or State University of New York at Albany (SUNY). The MESTSTAT model is based on the estimates from meteorological data and statistical modifications. The SUNY model derives solar radiation measurements from image brightness data and averaged ancillary data. The MESTSTAT model is based on the estimates from meteorological data and statistical modifications. Hourly solar radiation data modeled by both SUNY model and MESTSTAT model are available at NSRDB website and cover almost whole United States from 1990 to 2014 [16].

Daily average wind speed could be obtained from the Long-Term Pavement Performance (LTPP) database and National Climate Data Center (NCDC) database or the other meteorological network in each state. Even though the accurate site-specific daily average wind speed is preferred, the interpolation between close locations is accepted to make if site-specific daily average wind speed data cannot be obtained in the meteorological database. That is because the pavement temperature model is not extremely sensitive to the wind speed and the daily average values are adequate [16].

Hourly air temperature data could be collected from NCDC database. The following steps have been made to collected hourly air temperature data at various locations in the United States from NCDC database (http://www.ncdc.noaa.gov/).

1) Go to NCDC database homepage;
2) Go to Data Access;
3) Go to Quick Link;
4) Find number 3 resources (Integrated Surface Data, Hourly, Global); and
5) Select ISD/CDO.

Even though the hourly air temperature data could be obtained from NCDC database, several attempts show that some hourly air temperature data at various location collected from NCDC database are inadequate and unavailable for specific locations. Thus, the reasonable prediction of the hourly air temperature are required for accurate pavement temperature computation. A method was developed to predict the hourly air temperature based on daily average air temperature, daily maximum air temperature, and daily minimum air temperature. A conventional method to calculate hourly air temperature is to fit a sinusoidal function to predict the temperature variations [7, 11]. Nevertheless, the hourly air temperature profiles are not exactly sinusoidal shape. Therefore, a more accurate estimates of air temperature is required to implement the non-sinusoidal pattern. An imputation approach had been developed to determine the hourly air temperature. The representative pattern of daily air temperatures over a whole year is supposed to be determined firstly by using time series analysis of a seasonal trend decomposition [12]. This pattern could be used to construct the hourly air temperature depending on daily maximum air temperature, daily minimum air temperature, and daily average air temperature, which are collected from the LTPP database. The following steps is to locate these daily air temperature information in LTPP database (https://infopave.fhwa.dot.gov/).

1) Go the LTPP homepage;
2) Go to Data;
3) Go to Data Selection and Download;
4) Go to Climate
5) Check the "Show Advanced Data Classification" button; and
6) Select the "daily" under the "Temperature" and "VWS".

In order to determine an accurate estimate of pavement temperature based on the temperature mode, numerical values need to be interpolated from the collected site-specific pavement parameters from NCDC or NSRDB database, including albedo, emissivity, thermal diffusivity, absorption coefficient, and model parameters (a and d).

3.2 Prediction of Viscoelastic Thermal Stress

The top-down cracking of asphalt pavement layers are significantly affected by thermal stress and binder aging effects. Primarily, the thermal and aging effects would accelerate the initiation propagation process of these top-down cracks. The thermal stress in the pavement structure is the result of temperature variation. The pavement temperature with depth detailed in the above part will contribute to the computation of thermal stress in the pavement structure. This part would focus on the computation of viscoelastic thermal stress in the asphalt pavement layers. The aging of asphalt binder will also be taken into account for the computation of viscoelastic thermal stress.

In order to determine the viscoelastic thermal stress, the dynamic modulus data was used to determine the relaxation modulus and shift factor at specific time for computation of the thermal stress of asphalt pavement layers. The Dynamic modulus data for the selected pavement sections in each climate zone are collected from LTPP database to develop the master curve for different temperature. The climate zone constitutes the Wet-Freeze (WF) zone, Wet-None-Freeze (WNF) zone, Dry-Freeze (DF) zone and Dry-None-Freeze (DNF) zone. It is known that the asphalt mixture was viscoelastic materials. The master curve is used to determine the time-temperature mechanical properties of linear viscoelastic materials at a reference temperature. The room temperature, 20°C is used in this study as a reference temperature. The dynamic modulus master curve is constructed by using the sigmoidal function described in following equation [3].

$$\log E(t_r) = c_1 + \frac{c_2}{1+e^{c_3+c_4 \log t_r}} \tag{10}$$

where

E	=	the dynamic modulus;
c_1	=	the minimum value of the logarithm of dynamic modulus;
$c_1 + c_2$	=	the maximum value of the logarithm of dynamic modulus;
c_3, c_4	=	the parameters describing the shape of the sigmoidal function; and

t_r = the reduced time and inverse of reduced frequency of loading.

In the master curve of dynamic modulus determined by the concept of time-temperature superposition, the dynamic modulus is determined by replacing real time with reduced time according to following equation.

$$t_r = \frac{t}{a_T} \tag{11}$$

where

t_r = the reduced time and inverse of reduced frequency of loading;

t = the real time; and

a_T = the temperature shift factor;

The shift factor is determined by using the Arrhenius model, as shown in the below equation.

$$\log a_T = \frac{Ea}{R}\left(\frac{1}{T} - \frac{1}{T_0}\right) \tag{12}$$

where

Ea = activity energy (regarded as a fitting parameter);

R = universal gas constant;

T = test temperature, K; and

T_0 = reference temperature, K;

The relaxation modulus data are determined by converting the dynamic modulus data. The Prony series form of a relaxation modulus is assumed as presented in below equation. The coefficients of the Prony series are determined by fitting the constructed dynamic modulus master curve. The equation 13 and 14 are utilized to accomplish this conversion between the relaxation modulus and the dynamic modulus.

$$E(t) = \sum_{i=1}^{N} E_i e^{\frac{-t}{\lambda_i}} \tag{13}$$

where

E(t)	=	the relaxation modulus at reduced time t;
E_i, λ_i	=	the Prony series parameters for relaxation modulus curve.

$$\left|E^*(\omega)\right| = \sqrt{\left(\sum_{j=1}^{N} \frac{\omega^2 \lambda_j^2 E_j}{1+\omega^2 \lambda_j^2}\right) + \left(\sum_{j=1}^{N} \frac{\omega \lambda_j E_j}{1+\omega^2 \lambda_j^2}\right)} \tag{14}$$

Where

$E^*(\omega)$	=	the dynamic modulus at the angular frequency ω;
E_i, λ_i	=	the Prony series parameters.

The thermal stress in a pavement is computed according to the below constitutive equation 15, which is the Boltzamann's Superposition Principle for linear viscoelastic materials. The time-temperature dependent relaxation modulus of the asphalt mixture is required to compute the thermal stress. The finite different solution has been developed [13] by using the Prony series representation of E(ξ). This finite different solution is presented in equation 16.

$$\sigma(\xi) = \int_0^{\xi} E(\xi - \xi') \frac{d\xi}{d\xi'} d\xi' \qquad (15)$$

where

σ (ξ)	=	thermal stress at reduced time ξ;
E(ξ- ξ')=		the relaxation modulus at reduced time ξ- ξ';
ε	=	the strain at reduced time ξ(=α(T(ξ')-T));
α	=	linear coefficient of thermal contraction;
T(ξ')	=	pavement temperature at reduced time ξ';
T_0	=	pavement temperature when σ=0; and
ξ'	=	the variable of integration;

$$\sigma_i(t) = e^{-\Delta\xi/\lambda_i} \sigma_i(t - \Delta t) + \Delta\varepsilon E_i \frac{\lambda_i}{\Delta\xi}\left(1 - e^{-\Delta\xi/\lambda_i}\right) \qquad (16)$$

where

Δε	=	the changes in strain;
Δξ	=	the changes in reduced time;

Furthermore, the aging of asphalt binder will be taken into account for more accurate computation of thermal stress in asphalt pavement layers with time. It is known that dynamic modulus of asphalt mixture will increase due to the aging effect. However, most researchers didn't consider the aging effect on the computation of thermal stress in asphalt pavement layers. The rheological activation energy approach [9] has been accepted in this study to model the aged modulus for further calculating the thermal stress with regard to unavailable aged dynamic modulus data in the online database. The procedures of computation of thermal stress with consideration of the aging effect are summarized as follows.

Firstly, aged viscosity of an asphalt binder is determined in the following equation.

$$\eta = A_r e^{\frac{E_{ar}}{RT}} \quad (17)$$

where

η	=	the bitumen viscosity;
A_r	=	the rheological pre-exponential factor;
E_{ar}	=	the rheological activation energy of an asphalt binder; and
T	=	the absolute temperature;

Secondly, Witczak's predictive dynamic modulus model is utilized in this study to characterize the aged dynamic modulus of asphalt mixture, which is provided in the following equation [21].

$$\log E = -1.25 + 0.029P_{200} - 0.0018(P_{200})^2 + 0.0028P_4 - 0.058V_a - 0.822 * \frac{V_{beff}}{(V_{beff} + V_a)} + \frac{\left[3.872 - 0.0021P_4 + 0.004P_{38} - 0.00017(P_{38})^2 + 0.0055P_{34}\right]}{1 + e^{(-0.603313 - 0.3133511 \log f - 0.393532 \log \eta)}} \quad (18)$$

where

E	=	asphalt mixture dynamic modulus, in 10^5 psi;
η	=	bitumen viscosity, in 10^6 posie;

f = load frequency, in Hz;

V_a = percent of air voids in the mixture %, by volume;

V_{beff} = percent of effective asphalt content %, by volume;

P_{200} = percent of aggregate passing #200 sieve;

P_4 = percent of aggregate retained #4 sieve;

$P_{3/8}$ = percent of aggregate retained in 3/8 inch sieve;

$P_{3/4}$ = percent of aggregate retained in 3/4 inch sieve;

Thirdly, construct the master curve by using the sigmoidal function described in equation 11 based on the aged dynamic modulus data.

Fourthly, convert dynamic modulus to relaxation modulus by using the Prony series model described in the equation 13 and 14.

Fifthly, the aged relaxation modulus is used in computation of thermal stress in the asphalt pavement layers.

The simple flow chart of the computation of the viscoelastic thermal stress in the asphalt pavement layers is depicted in the following figure based on the original condition and aging effect.

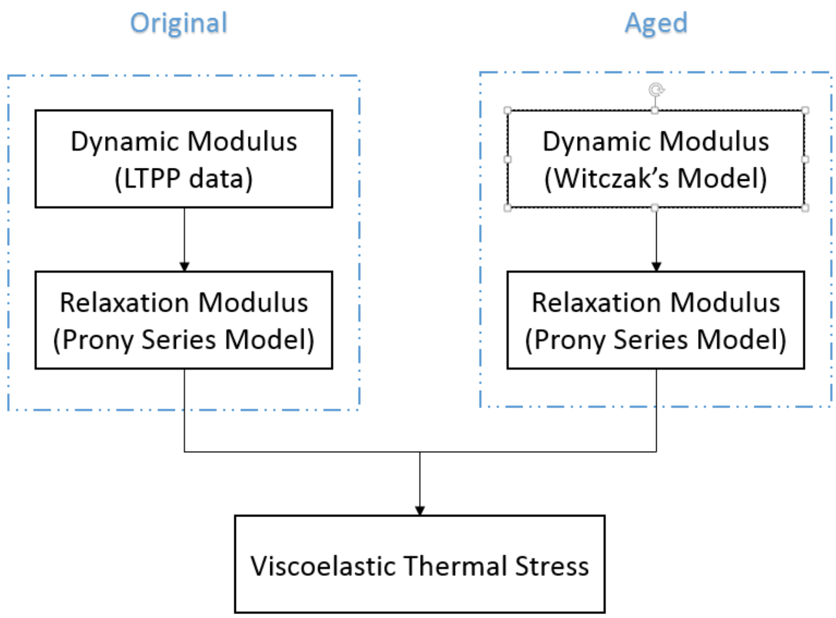

Figure 3. Process of the Computation of Viscoelastic Thermal Stress

3.3 Prediction of Viscoelastic Thermal Cracking

3.3.1 Viscoelastic Thermal-Related Top-down Cracking Model

The viscoelastic thermal crack model is developed in this study based on the Paris' Law for crack propagation. The Paris' Law is commonly used to characterize the fracture growth and predict the change in the depth of a crack subject to a cooling cycle, provided in the equation 19. In this study, the top-down cracking of asphalt pavement layers under thermal loading is considered primarily in the vertical pavement structure, as shown in the figure 4.

$$\Delta c = A(\Delta K)^n \text{ or } \Delta c = A(J_R)^n \quad (19)$$

where

ΔC	=	change in crack depth due a cooling cycle;
ΔK	=	change in the stress intensity factor due a cooling cycle;
J_R	=	pseudo J-integral; and
A, n	=	fracture parameters for the asphalt mixture

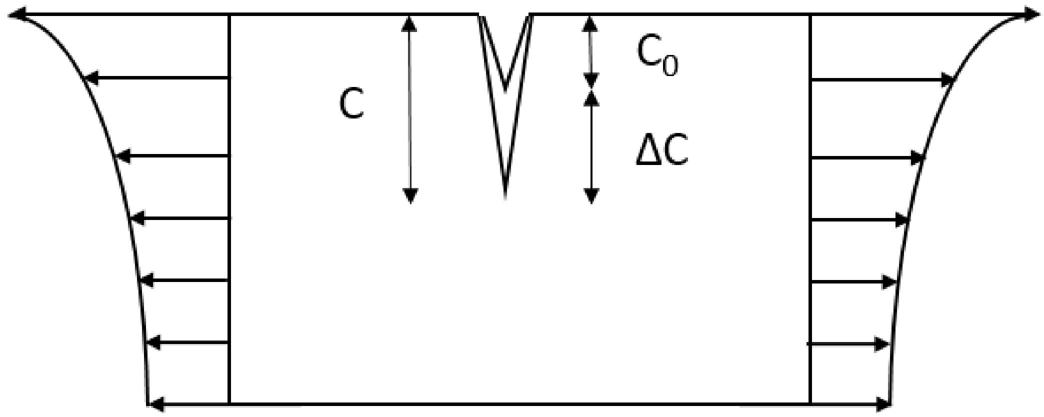

Figure 4. Schematic of Crack Depth Model [22]

The value of K in the above equation is stress intensity factor that is used to predict the stress state near the crack tip. The J-integral is the way to calculate energy release rate due to the crack growth. The fracture mechanical model using Paris' Law is used to predict the crack propagation of viscoelastic, viscoplastic, viscofracturing material type like asphalt mixture in this study. By the definition, K is formulated and applied to the linear elastic material and J is applied to the elastic plastic fracture materials [14]. Pseudo J-integral is preferred to be adopted in this study. A conversion from K to J_R is presented in the following relationship [14].

$$J_R = \frac{1-\upsilon^2}{E_R}\left(K_1^2 + K_2^2\right) + \frac{1-\upsilon^2}{E_R} K_3^2 \tag{20}$$

where

J_R	=	pseudo J-integral;
υ	=	Poisson's ratio;
K_1	=	the Mode 1 (opening) stress intensity factor;
K_2	=	the Mode 2 (in-plane shear) stress intensity factor;
K_3	=	the Mode 3 (out of plane shear) stress intensity factor; and
E_R	=	reference modulus;

The reference modulus used in this study is determined by equation 20, which is referred to the representative elastic modulus [4]. The dynamic modulus and relaxation modulus data are required to determine the reference temperature. The dynamic modulus, $|E^*|$ is determined by equation 10 based on the constructed master curve (where $f = 1$ Hz). The relaxation modulus E used in equation 21 was developed as a simple power law model (where $t_p = 1$ s), presented in the equation 22. Relaxation modulus modeled by power law would be determined by the relaxation modulus data modeled by Prony series equation 13.

$$E_{re} = \frac{1}{2}\left[\left|E^*\right|_{f=\frac{1}{t_p}} + E\left(t = \frac{t_p}{2}\right)\right] \tag{21}$$

where

E_{re}	=	reference modulus (representative elastic modulus);

$|E^*|$ = dynamic modulus at the frequency of f; and

E = relaxation modulus at the time of $t_p/2$.

$$E(t) = E_1 t^{-m} \tag{22}$$

where

E(t) = relaxation modulus at reduce time t; and

E_1, m = the coefficients of the relaxation modulus.

In the consideration of aging in the asphalt mixture, the dynamic modulus and relaxation modulus will increase with time. Thus, the reference modulus used in the calculation of crack growth would also increase with time. The kinetics-based aging prediction of the asphalt mixtures has been proposed in Luo et al [9] and used in this study for the calculation of aged reference modulus. The aged modulus has been modeled using the following equations.

$$E = E_i + (E_o - E_i)\left(1 - e^{-k_f t}\right) + k_c t \tag{23}$$

$$k_f = A_f e^{-\frac{E_{af}}{RT_a}} \tag{24}$$

$$k_c = A_c e^{-\frac{E_{ac}}{RT_a}} \tag{25}$$

Where

E_i = the initial modulus;

E_0 = the intercept of the constant-rate line of modulus;

E_{af} = the fast-rate aging activation energy for modulus;

E_{ac} = the constant-rate aging activation energy for modulus;

k_f = the fast-rate reaction constant for modulus;

A_f = the fast-rate pre-exponential factor for modulus;

k_c = the constant-rate reaction constant for modulus;

A_c = the constant-rate pre-exponential factor for modulus;

R = universal gas constant value.

T_a = the aging absolute temperature;

3.3.2 Determination of Fracture Parameters by Performance-related Properties

The fracture parameters A and n are related to the cracking performance. The determination of A and n depends on the performance-related material properties. In this study, it is considered that relaxation modulus, air voids content, asphalt binder content, aggregate gradation characteristics are mostly used for asphalt pavement design and related to the asphalt pavement performance. Thus, these performance-related material properties are used to determine the fracture parameters, A and n.

These performance-related material properties can be obtained from LTPP database. The following steps have been made to collect material properties at various locations in the United States from LTPP database (https://infopave.fhwa.dot.gov/).

1) Go the LTPP homepage;
2) Go to Data;
3) Go to Data Selection and Download;
4) Go to Structure

5) Check the “Show Advanced Data Classification” button; and

6) Select the “AC Mixture Properties” under the “AC” and “Material”.

7) Select the “AC Mixture Properties (Test Results – Asphalt Concrete)” under the “AC” and “Material”.

The step 6 mentioned above is taken to collect the air voids content, asphalt binder content data and aggregate gradation data. The step 7 shown above is access to dynamic modulus data at different pavement sections. The dynamic modulus data obtained herein would be used to convert relaxation modulus. The aggregate gradation data collected herein would be used to fit the curve of the cumulative percentage passing versus the sieve size using an appropriate power law function, as shown below [2].

$$f\left(x\right)=\theta x^{\phi} \tag{26}$$

where

$f(x)$	=	cumulative percent passing;
x	=	sieve size;
θ	=	the aggregate scale parameter; and
ϕ	=	the aggregate shape parameter.

The fracture parameters, A and n, are determined by equations 27 and 28 based on Luo’s work [2]. The relationship between the logarithm of A and n was identified as a power relation, as shown in equation 27. The relationship between the n value and selected performance-related material properties was conducted based on multiple regression analysis, as provided in equation 28.

$$A = 10^{-(1.246n+3.615)} \quad (27)$$

where

A, n	=	fracture parameters.

$$n = -16.052 + 0.135AV\% + 6.500\ln\left(AB\%\right) + 8.147\phi + 5.512\frac{1}{m} - 81.515\left(\frac{1}{E_1}\right)^m \quad (28)$$

where

n	=	fracture parameter;
AV%	=	air voids content of asphalt mixture;
AB%	=	asphalt binder content of asphalt mixture;
ϕ	=	the aggregate shape parameter; and
E_1, m	=	the coefficients of the relaxation modulus.

3.3.3 Procedure to Predict Cracking under Thermal Loading

In this study, the total amount of 63 sections in four climate zones are selected from LTPP database to predict top-down cracking of asphalt pavement layers under thermal loading. Then the traffic-related top-down cracking will be determined with combination of thermal-related cracking for field calibration in future work. The procedure to predict thermal-related top-down cracking is elaborated as follows.

1) Collect the required climate data from LTPP and NSRDB database, including daily maximum and minimum air temperature, daily average temperature, daily wind speed, hourly solar radiation.

2) Interpolating the site-specific pavement temperature model parameters with collected data from NCDC or NSRDB database, including albedo, emissivity, thermal diffusivity, absorption coefficient, and the pavement parameter (a and d).
3) Calculate the hourly pavement temperature based on pavement temperature model.
4) Obtain the material properties data from LTPP database, including the raw dynamic modulus data, binder content, air void content, and aggregate gradation.
5) Calculate the reference modulus and relaxation modulus, which are related to the dynamic modulus collected from LTPP database.
6) Calculate the thermal stress over time for each selected pavement section by using equation 16.
7) Calculate the J-integral using the calculated reference modulus and thermal stress by equation 20, in which the Poisson ratio, υ is assumed to be 0.3; the K_2 and K_3 are assumed to be zero; and K_1 is determined by the equation 29 [14].
8) Calculate the fracture parameters, A and n by obtaining the performance-based material properties, as shown in equation 27 and 28.
9) The initial crack length is assumed to be the average air void size. The regression relation between initial crack length and the air void content is shown in equation 30 [15].

10) The crack increment due to the temperature variation (1 cycle = 1 hour) is calculated by equation 19.

11) Calculate the average crack size over time by using equation 31.

$$K_1 = 2\sigma^{\infty}\sqrt{\frac{c}{\pi}} \tag{29}$$

where

K_1	=	the Mode 1 (opening) stress intensity factor;
σ^{∞}	=	remote stress in a uniforms state;

$$c_0 = 0.0037(AV\%)^2 + 0.0071(AV\%) + 0.5583 \tag{30}$$

$$c_i = c_{i-1} + A(J_{Ri-1})^n \tag{31}$$

4 RESULTS AND ANALYSIS

This chapter details one case study of prediction of top-down cracking in asphalt pavement layers under thermal loading. The results of pavement temperatures, dynamic modulus master curves, relaxation modulus, unaged and aged thermal stress, and material properties are elaborated and analyzed as follows.

4.1 Pavement Temperature

One case study for estimating the top-down cracking in asphalt pavement layers under thermal loading would be elaborated in this chapter. One of the SHRP sections from LTPP database is taken as an example for the proposed mechanical-empirical approach of prediction of thermal-dependent top-down cracking. The example of SHRP section is 27-1018, which is located at Morrison, Minnesota and in the Wet-Freeze (WF) climate zone. The proposed approach for an estimate of thermal-dependent top-down cracking is schematically depicted in the figure 5. It is shown in the below flow chart that pavement temperature is determined firstly in order to compute the viscoelastic thermal stress based on the collected, daily wind speed, hourly solar radiation, hourly air temperature and site-specific pavement parameters. Table 1 presents the collected pavement parameters of emissivity coefficient, absorption coefficient, albedo, a and d.

Moreover, the climate data of this section within a period of 26 years from 1984 to 2010 have been collected from online database. The hourly solar radiation over 26 years have been collected from NSRDB database regarding to the corresponding climate station close the selected SHRP section. The daily wind speed data have been obtained from the LTPP database. The maximum, minimum and average air temperature data have been gathered from the LTPP database. The representative pattern of daily air temperature over a whole year is determined using time series analysis of a seasonal trend decomposition, which is a statistical approach as implemented in the function stl in Software R. This pattern is used to construct the hourly air temperatures based on these collected air temperature data.

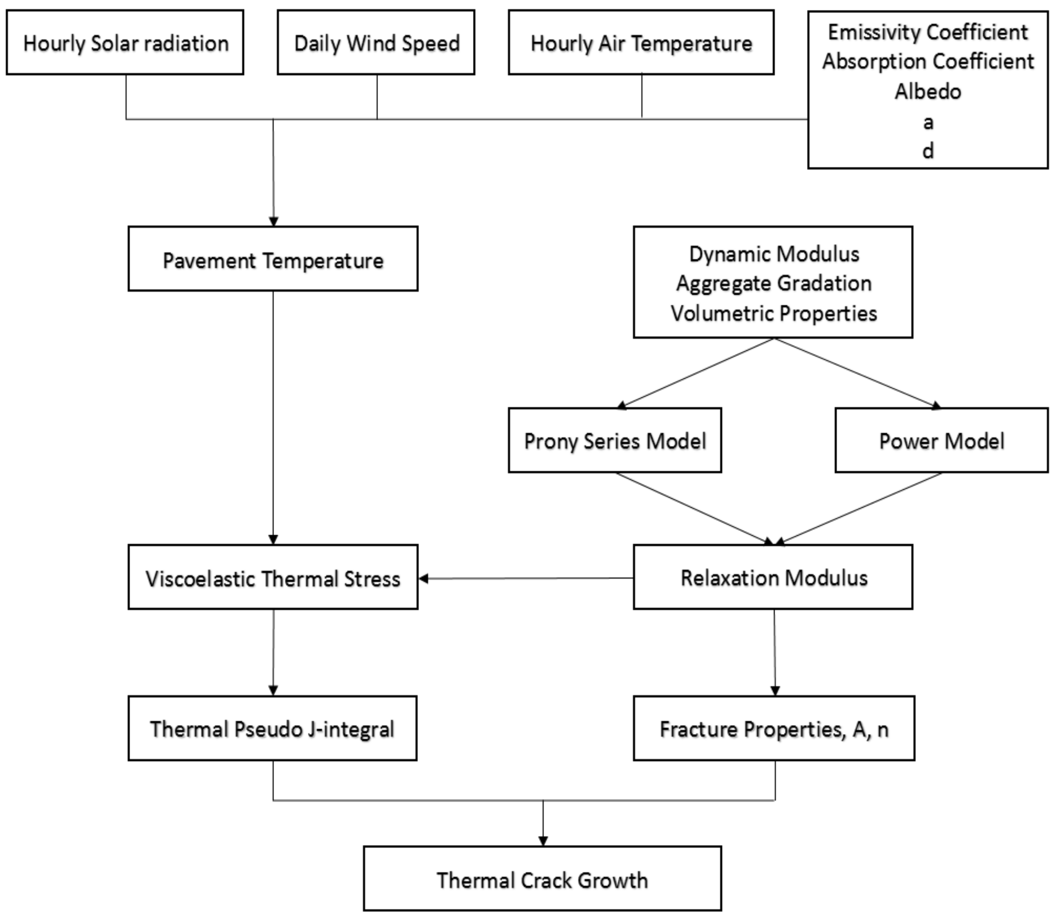

Figure 5. Flow Chart of the Process of the Thermal Crack Growth Computations

Table 1. Thermal Coefficients

Emissivity Coefficient	Absorption Coefficient	Albedo	a	d
0.8	0.75	0.3	1.4	0.5

Based on the collected climate data and site-specific thermal coefficients, the pavement temperature of this section has been determined by using the pavement temperature model as implemented in the software Visual Studio by using the C# programming language. The results of pavement temperature over a period of 1984 to 1987 are shown in the figure 6. Obviously, it could be seen that this pavement section suffered an extremely severe winder over years and the lowest pavement temperature is less than -30℃. It illustrates that the low temperature could be regarded as one of the primary cause for the development of top down cracking.

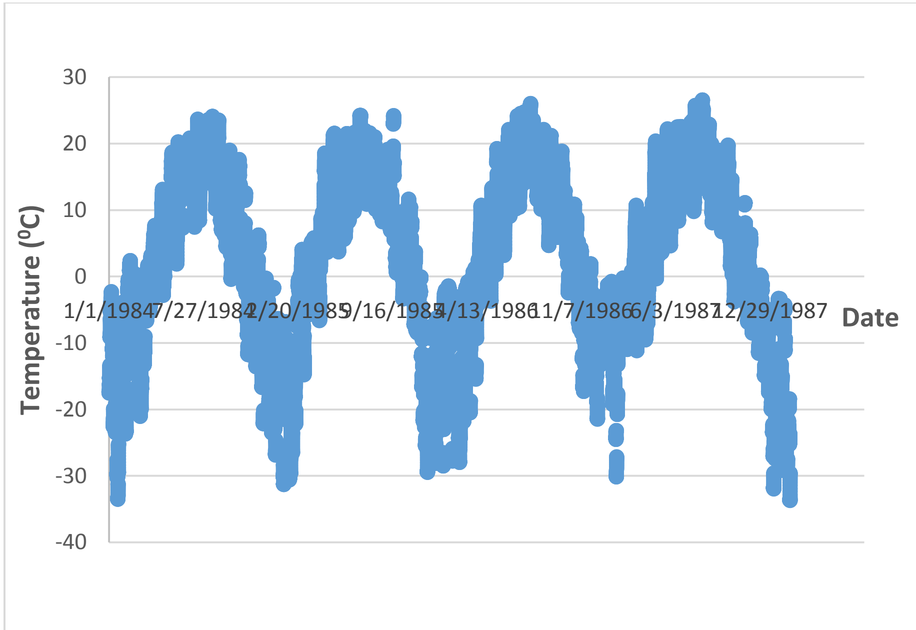

Figure 6. Pavement Temperature versus Time

4.2 Dynamic Modulus Master Curve

Table 2 presents the dynamic modulus data that collected from the LTPP website. These dynamic modulus presented below is at five temperatures (14 °F, 40 °F, 70 °F, 100 °F, 130 °F) and six loading frequencies (0.1 Hz, 0.5 Hz, 1 Hz, 5 Hz, 25 Hz). The Arrhenius model described in the equation 12 has been used to determine shift factor at five temperatures, as shown in the figure 7. It could be seen that shift factor decease with the increasing temperature. The sigmoidal model presented in the equation 10 have been used to construct the dynamic modulus master curve, as shown in the figure 8. It can be seen in the figure 6 that the sigmoidal model data almost perfectly match the laboratory dynamic modulus data collected from LTPP database. The table 3 provides the sigmoidal model and Arrhenius model fitting parameters.

Table 2. Original Dynamic Modulus Data from LTPP

Frequency, Hz	E* (Psi)				
	Temperature, F				
	14	40	70	100	130
0.1	2417611	998437	189391	42172	17947
0.5	2765339	1394039	322960	67610	24447
1.0	2896924	1575382	402447	84197	28543
5.0	3159162	1999087	646456	143464	43024
10.0	3254195	2175762	777748	181287	52407
25.0	3364591	2398333	973652	246546	69156

Table 3. Master Curve Coefficients

c1	c2	c3	c4	Ea
4.43	-2.49	0.423	-0.500	100756

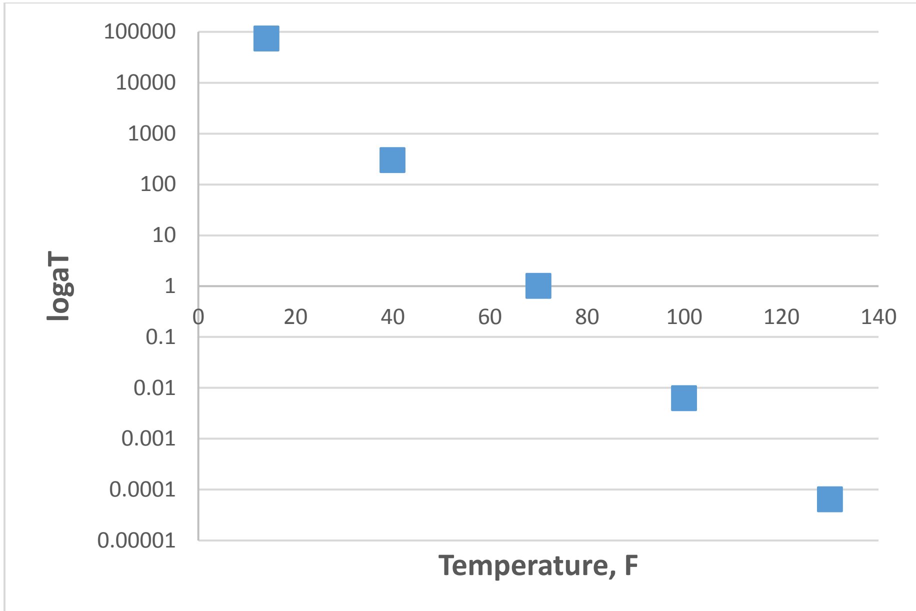

Figure 7. Shift Factor versus Temperature

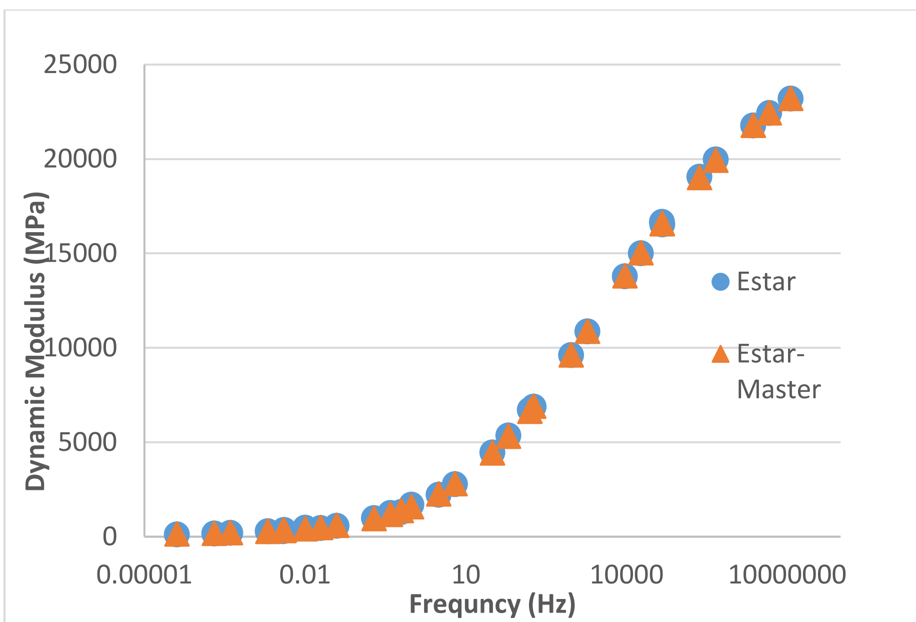

Figure 8. Dynamic Modulus Master Curve Based on Sigmoidal Model

In terms of the constructed dynamic modulus master curve using the sigmoidal model, the coefficients in Prony series model of relaxation modulus have been determined by fitting the master curve as shown in the figure 8. The equation 14 is used to construct the master curve of relaxation modulus, involving the Prony series coefficients. The more Prony series coefficients are selected, more accurate the relaxation modulus is calculated using Prony series model. Thus, thirty sets of Prony series coefficient are chosen in this study. Table 4 presents calculated the Prony series coefficients for the selected section.

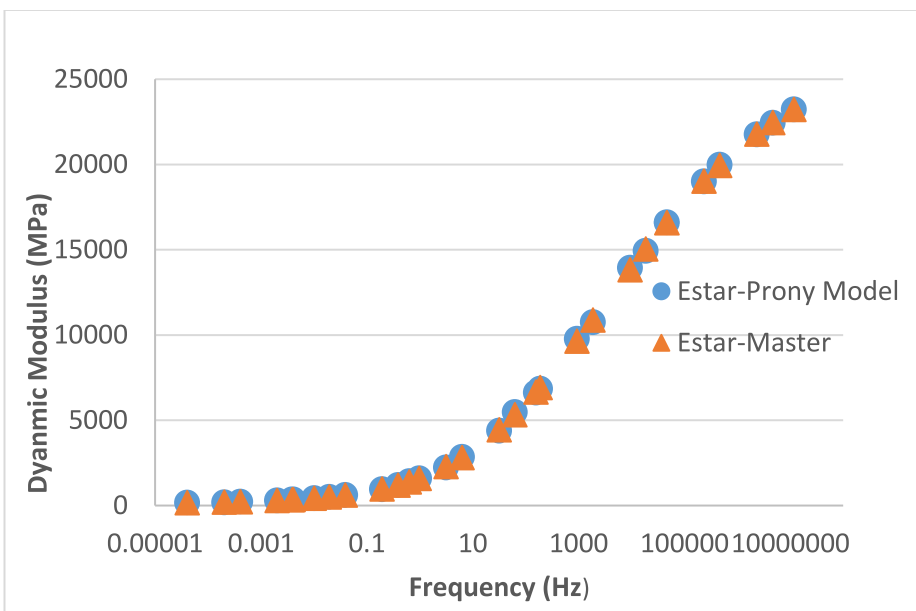

Figure 9. Dynamic Modulus Master Curve Based on Prony Series Model

Table 4. Prony Series Model Coefficients

E_i (MPa)		Retardation Time (sec)	
$\mathbf{E_1}$	710.0050896	$\boldsymbol{\lambda_1}$	2.00E-14
$\mathbf{E_2}$	710.0289252	$\boldsymbol{\lambda_2}$	2.00E-13
$\mathbf{E_3}$	710.2941641	$\boldsymbol{\lambda_3}$	2.00E-12
$\mathbf{E_4}$	720.1170417	$\boldsymbol{\lambda_4}$	2.00E-11
$\mathbf{E_5}$	1283.744622	$\boldsymbol{\lambda_5}$	2.00E-10
$\mathbf{E_6}$	721.3749882	$\boldsymbol{\lambda_6}$	2.00E-09
$\mathbf{E_7}$	1.41E-05	$\boldsymbol{\lambda_7}$	2.00E-08
$\mathbf{E_8}$	1930.238772	$\boldsymbol{\lambda_8}$	2.00E-07
$\mathbf{E_9}$	3018.999623	$\boldsymbol{\lambda_9}$	2.00E-06
$\mathbf{E_{10}}$	4024.928809	$\boldsymbol{\lambda_{10}}$	2.00E-05
$\mathbf{E_{11}}$	4352.227319	$\boldsymbol{\lambda_{11}}$	2.00E-04
$\mathbf{E_{12}}$	3992.908436	$\boldsymbol{\lambda_{12}}$	2.00E-03
$\mathbf{E_{13}}$	3059.513012	$\boldsymbol{\lambda_{13}}$	2.00E-02
$\mathbf{E_{14}}$	1533.448385	$\boldsymbol{\lambda_{14}}$	2.00E-01
$\mathbf{E_{15}}$	858.6732468	$\boldsymbol{\lambda_{15}}$	2
$\mathbf{E_{16}}$	282.9135338	$\boldsymbol{\lambda_{16}}$	20
$\mathbf{E_{17}}$	133.0550007	$\boldsymbol{\lambda_{17}}$	200
$\mathbf{E_{18}}$	109.1621086	$\boldsymbol{\lambda_{18}}$	2000
$\mathbf{E_{19}}$	0.753299441	$\boldsymbol{\lambda_{19}}$	20000
$\mathbf{E_{20}}$	6.5044783	$\boldsymbol{\lambda_{20}}$	2.00E+05
$\mathbf{E_{21}}$	2.58E-05	$\boldsymbol{\lambda_{21}}$	2.00E+06
$\mathbf{E_{22}}$	2.58E-05	$\boldsymbol{\lambda_{22}}$	2.00E+07
$\mathbf{E_{23}}$	2.58E-05	$\boldsymbol{\lambda_{23}}$	2.00E+08
$\mathbf{E_{24}}$	2.58E-05	$\boldsymbol{\lambda_{24}}$	2.00E+09
$\mathbf{E_{25}}$	2.61E-05	$\boldsymbol{\lambda_{25}}$	2.00E+10
$\mathbf{E_{26}}$	2.60E-05	$\boldsymbol{\lambda_{26}}$	2.00E+11
$\mathbf{E_{27}}$	6.021536141	$\boldsymbol{\lambda_{27}}$	2.00E+12
$\mathbf{E_{28}}$	67.00108037	$\boldsymbol{\lambda_{28}}$	2.00E+13
$\mathbf{E_{29}}$	93.3016193	$\boldsymbol{\lambda_{29}}$	2.00E+14
$\mathbf{E_{30}}$	2.105507334	$\boldsymbol{\lambda_{30}}$	2.00E+15

4.3 Results of Thermal Stress

The thermal stress in asphalt pavement layers is computed according to the equation 16. One program has been developed in Visual Studio software and C# computer language to calculate the hourly thermal stress based on computed hourly pavement temperature, shift factors and Prony series coefficients. The computed unaged hourly thermal stress over 5 years is shown in following figure. The unaged hourly thermal stress is computed without the consideration of age effect on the relaxation modulus. In other words, the original dynamic modulus data are used to compute thermal stress with aging time. It can be observed from the figure 10 that hourly thermal stress exhibits a high value in the winter and extremely minor value in the summer, additionally illustrating that low temperature has a paramount effect on the thermal stress and high temperature effect could be ignored.

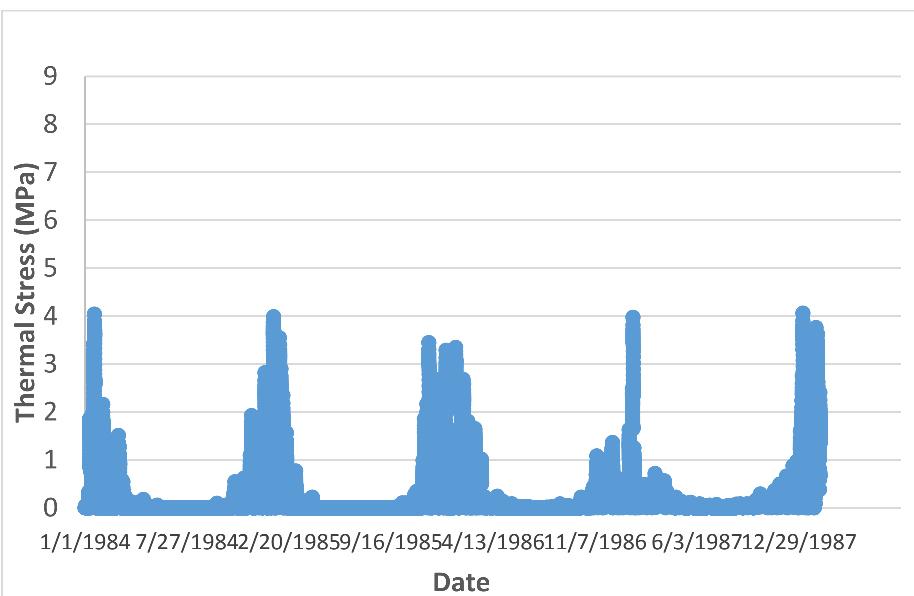

Figure 10. Unaged Thermal Stress versus Time

In addition to the unaged thermal stress, the aging of asphalt mixture is taken into account for more accurate computation of thermal stress in asphalt pavement layers with time in this study. The rheological activation energy approach has been accepted to model the temperature-dependent dynamic modulus for further calculating the thermal stress. The regression relationship between rheological activation energy of asphalt binder and aging time is represented in the figure 11. Moreover, the regression relation between rheological pre-exponential factor and rheological activation energy is shown in the figure 12. These regression relationships are referred to Luo et al. [9]. Both of these regression relationships are only suitable in the Wet-Freeze (WF) climate zone. According to the equation 18, the aged viscosity of an asphalt binder with aging time is determined based on these two regression relationships under five temperatures (14 °F, 40 °F, 70 °F, 100 °F, 130 °F). Furthermore, the aged dynamic modulus is determined using empirical dynamic modulus model presented in the equation 18 based on the aged viscosity at five temperature. The loading frequency used in equation 18 are 0.1 Hz, 0.5 Hz, 1 Hz, 5 Hz and 25 Hz in order to correspond the original laboratory dynamic modulus data from LTPP database. The other parameters in equation 18 are material properties, as shown in the table 5 and 6. The aged dynamic modulus master curve and aged relaxation modulus using Prony series model are established for computation the aged thermal stress, as shown in the figure 13.

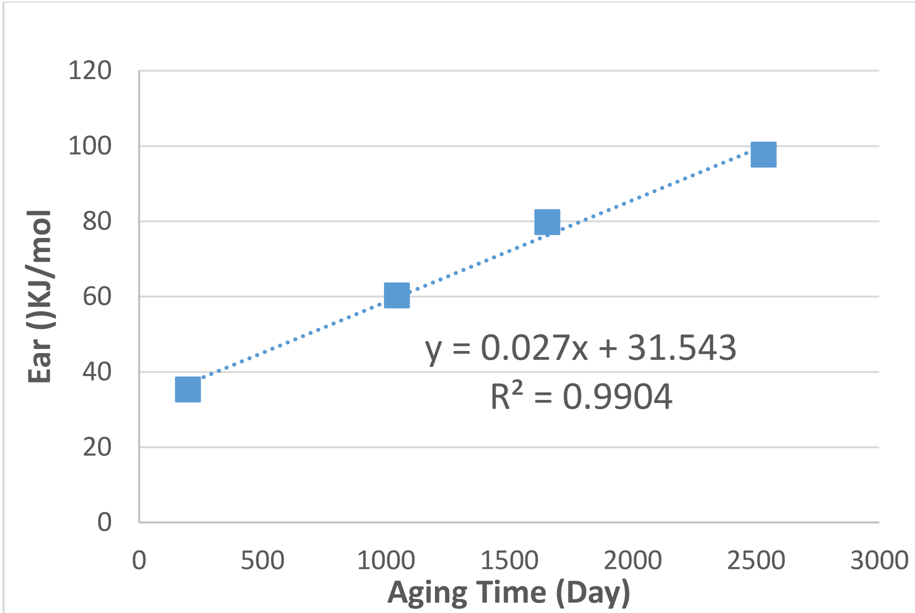

Figure 11. Activation Energy for Viscosity versus Time

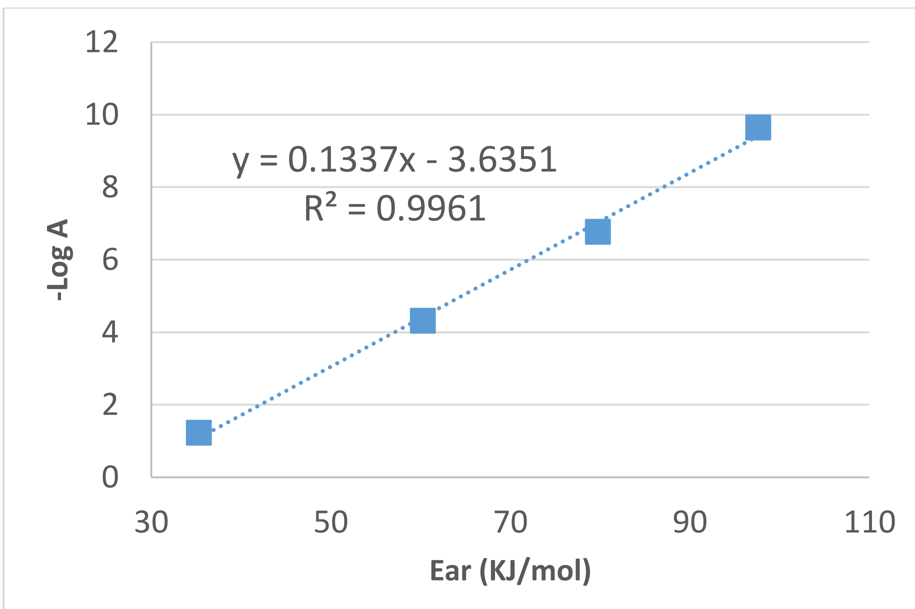

Figure 12. Relation between the Ear and –LogA

The calculated results of aged thermal stress with aging time are larger than the unaged thermal stress, comparing with the figure 10 and 13. It is observed from the figure 10, the maximum thermal stress is larger than 4 MPa at the temperature less than -30℃. However, it is seen from the figure 13 that the maximum aged thermal stress is larger than 7MPa during winter. Therefore, the difference between the unaged and aged thermal stress is not supposed to be ignored. Consideration of aging effect of asphalt binder for computation of thermal stress in asphalt pavement layers should be more acceptable for most research works.

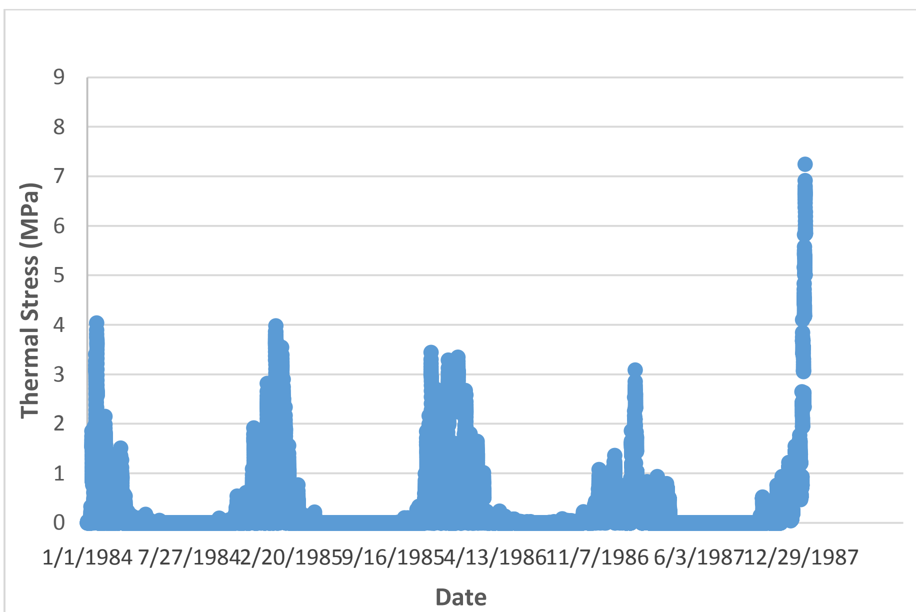

Figure 13. Aged Thermal Stress versus Time

4.4 Results of Thermal-Related Top-Down Cracking

Prior to compute the thermal-related top-down crack growth with time, the fracture parameter in the equation 19 should be determined given the material properties, as shown in the equation 27 and 28. The table 5 presents the selected section information and corresponding material properties, including the air voids, asphalt content, and aggregate parameter obtained from LTPP database. The table 6 represents the aggregate gradation that can be used to fit the curve of the cumulative percentage passing versus the sieve size using an appropriate power law function in the equation 26. The aggregate shape parameter, ϕ is presented in table 5.

Table 5. Section Information and Material Properties.

State Name	Minnesota
County Name	Morrison
SHRP ID	27-1018
Climate Zone	WF
BSG*	2.391
Gmm**	2.452
Air Voids (%)	2.49
Asphalt Content (%)	5.5
Aggregate Parameter (ϕ)	0.59

*: bulk specific gravity. **: maximum specific gravity.

Table 6. Aggregate Gradation (LTPP)

Sieve Size	Percent Passing by Weight (%)
1 in. (25mm)	100
3/4 in. (19mm)	100
1/2 in. (12.5mm)	93
3/8 in. (9.5mm)	84
No.4 (4.75mm)	70
No. 10 (2mm)	54
No. 40 (0.425mm)	18
No. 80 (0.177mm)	6
No. 200 (0.075mm)	3.3

The other two parameters used for the computation of fracture parameters, A and n are E_1 and m that are used to characterize the relaxation modulus by power law function, as shown in the equation 22. The figure 14 illustrates that relaxation modulus in power law model is fitted by the one in Prony series model shown in the equation 12. Depending on the determined Prony series coefficients in the table 4, the parameters E_1 and m are determined as listed in the table 7. Therefore, fracture parameters are calculated using the regression functions in equation 27 and 28, as presented in table 7.

The Paris' law is used in this study to characterize the crack growth in the equation 19. Pseudo J-integral is the last variable to solve after the determination of two fracture parameters by a conversion from K to pseudo J-integral in the equation 20. Assuming that the Poisson ratio is 0.35 and both of K_2 and K_3 are assumed to be zero and K_1 is determined by the equation 28, the J-integral will be calculated by using calculated reference modulus and thermal stress.

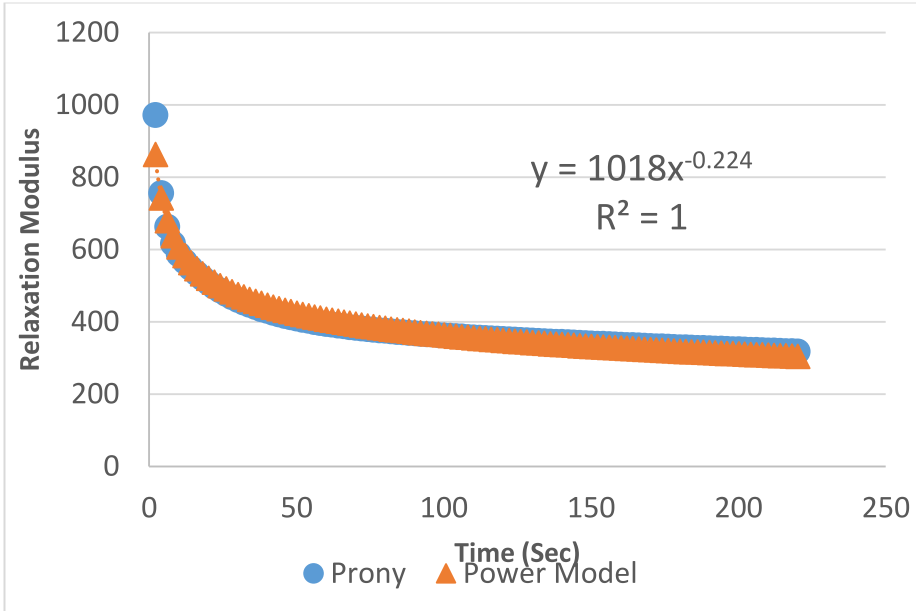

Figure 14. Relaxation Modulus versus Time Based on Power Model and Prony Series Model

Table 7. Fracture Parameters

E_1 (MPa)	m	E_{re}(MPa)	A	n
1018	0.224	1982	1.36772E-14	8.2255

The determination of thermal stress is taken consideration of aging effect of asphalt mixtures and is presented in the figure 13. The calculation of the reference modulus herein also considers the aging of asphalt mixture exhibiting the increase of modulus. The reference modulus in this study is determined by the equation 21 that is referred to the representative elastic modulus [4]. The dynamic modulus and relaxation modulus data are required to determine the reference modulus. The dynamic modulus, $|E^*|$ is determined by the equation 10 based on the constructed master curve (where $f = 1$ Hz), presented in the figure 8. The relaxation modulus E used in equation 21 was developed in the equation 21 as a simple power law model (where $t_p = 1$ s), presented in the figure 9. The original reference modulus value is shown in the table 7. Due to the consideration of aging in asphalt mixtures, the kinetics-based aging prediction of the asphalt mixtures has been proposed in Luo et al [9] and used in this study for the calculation of aged reference modulus using the equation 23.

In the equation 23, the initial modulus, fast-rate and constant-rate of aging activation energy and pre-exponential factors, the aging absolute temperature and intercept of the constant-rate line of modulus are required to achieve this kinetics-based aging prediction model. The initial modulus has been determined and presented in the table 7. The fast-rate and constant-rate of aging activation energy and pre-exponential factors for modulus are referred at Luo et al [9]. The hourly pavement temperature variations over years from 1984 to 1987 are calculated by the pavement temperature model in the developed computer program as a C# script file, as presented in the figure 6. The harmonic mean of the temperatures is proposed to be an appropriate value as the aging absolute temperature. That is because the aging temperature herein follows the Arrhenius kinetics. The harmonic mean could provide the truest and desired average of rates. The intercept of the constant-rate line of modulus is determined by separation of the modulus into constant-rate part and fast-rate part. The obtained aged reference modulus with aging time is illustrated in the figure 15. This shape of aged reference modulus with aging time is similar to the shape of pavement temperature with time in the figure 6, illustrating the reference modulus has similar variation of pavement temperatures. Furthermore, the reference modulus variation has increasing trend with aging time, as shown in the figure 15, in accordance to the field condition. That illustrates the importance of consideration of aging effect and more reasonable approach to determine the modulus with aging time.

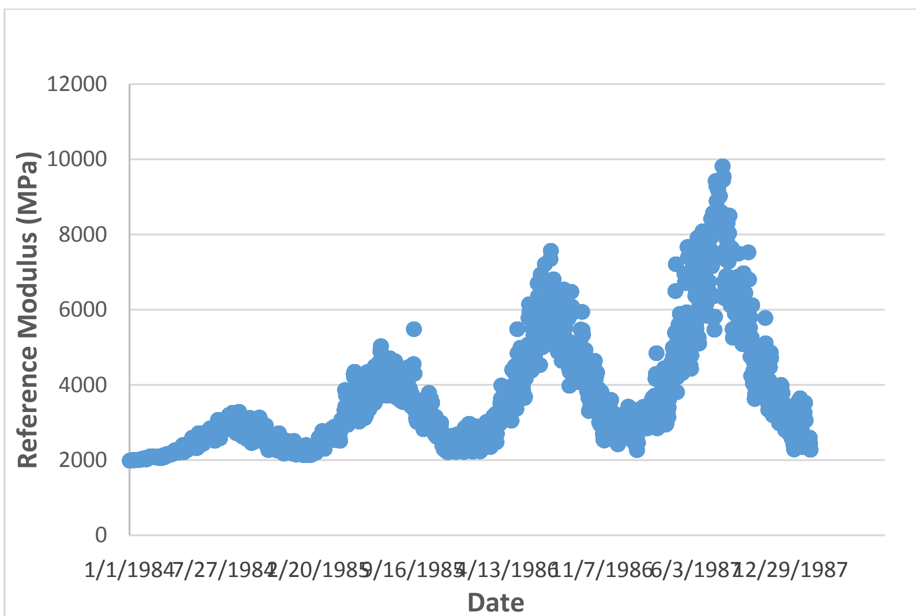

Figure 15. Aged Reference Modulus versus Time

After obtaining the aged reference modulus and thermal stress, the J-integral value has been determined using the equation 20. Therefore, the Paris' law could be used herein to characterize the crack growth in the equation 19. The initial crack length is assumed to be the regression relation between average air voids size and air void content, as illustrated in the equation 30. The average crack length over years is calculated using the equation 31. Therefore, the result of crack length over years is shown in the figure 16 for the selected pavement section 27-1018. It illustrates that under the influence of temperature variations approximate 4 years have been taken to propagate cracks from surface to the bottom of asphalt pavement layers for the selected pavement section 27-1018.

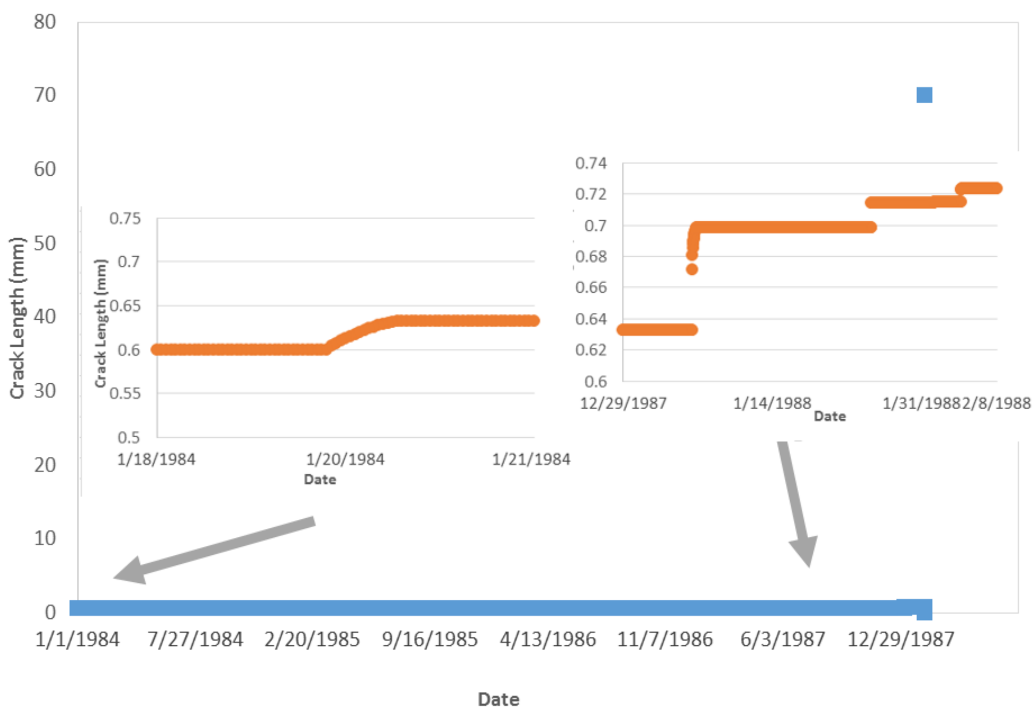

Figure 16. Crack Depth versus Time

5 CONCLUSIONS AND FUTURE RESEARCH

The objective of this study is to develop a mechanistic-empirical approach to predict the top-down cracking under thermal loading in the asphalt pavement layers. This protocol depends on modeling of pavement temperature, thermal stress and crack propagation. The aging effect of asphalt mixture is taken into consideration in this study for the calculation of reference modulus and thermal stress. The estimation of thermal-related top-down cracking is established using Paris law and implemented by a developed computer program in Visual Studio using C# language. The specific conclusions made in this study are as follows.

1. The pavement temperature model developed by the research group at Texas A&M University [1] is adopted in this study and shows a better estimation of temperature variation over time in asphalt pavement layers. The required climate data and site-specific pavement parameters for this pavement temperature model are accessible at some online database, such as NSRDB and LTPP. The pavement temperature model is implemented by a developed temperature program to predict the pavement temperature rapidly and conveniently.
2. The determination of viscoelastic thermal stress in asphalt pavement layers is according to a constitutive equation resolved by a finite difference solution. This solution is achieved by a developed thermal stress program to predict the hourly thermal stress. The Prony series coefficients and shift factors are

necessitated as inputs to the thermal stress program and obtained by the conversion of dynamic master curve and relaxation modulus on Prony series model. The rheological activation energy approach has been used in this study to predict the aging viscosity of binder for further envisioning aging modulus of asphalt mixtures which cannot be ignored in the computation of thermal stress.

3. The estimation of thermal-related top-down cracking in asphalt pavement layers is implemented by a developed crack propagation program. The prediction of crack growth is achieved by using Paris' law in which aging of reference modulus is taken into consideration to calculate the pseudo J-integral. The kinetics-based aging prediction approach is used in this study for the calculation of aged reference modulus.
4. The complete program is developed to accomplish the prediction of thermal-dependent top-down cracking in asphalt pavement in this study. The required inputs, such as climate data, dynamic modulus, material properties are approachable, showing a better availability and simplicity of this application.

Some future works for this study are detailed as follows.

1. This study focuses on the thermal influence on top-down cracking. The calibration of this proposed mechanistic-empirical approach of prediction of thermal-related top-down cracking would be accomplished with combination of traffic effect on top-down cracking in asphalt pavement layers in comparison with the field longitudinal cracks data.

2. The aging characterization and prediction is achieved using kinetic-based aging prediction model in this study, as referred to Luo et al. [9]. Nevertheless, more calibration and validation work are required to ensure a better accuracy of this aging prediction and more activation energy data for modulus and viscosity for four climate data and various pavement sections would be further investigated for a better and widespread applicability.
3. The considered aging effect in this study did not include the aging modulus with pavement depth.

REFERENCES

1. Lytton, R. L., Tsai, F. L., Lee, S. I., Luo, R., Hu, S., & Zhou, F. (2010). Models for predicting reflection cracking of hot-mix asphalt overlays (No. Project 01-41).
2. Luo, X., Zhang, Y., & Lytton, R. L. (2015). Implementation of pseudo J-integral based Paris' law for fatigue cracking in asphalt mixtures and pavements. Materials and Structures, 1-20.
3. Kim, Y. R., Underwood, B., Far, M. S., Jackson, N., & Puccinelli, J. (2011). LTPP computed parameter: dynamic modulus (No. FHWA-HRT-10-035).
4. Underwood, B. S., & Kim, Y. R. (2009). Determination of the appropriate representative elastic modulus for asphalt concrete. International Journal of Pavement Engineering, 10(2), 77-86.
5. Farrar, M. J., Hajj, E. Y., Planche, J. P., & Alavi, M. Z. (2013). A method to estimate the thermal stress build-up in an asphalt mixture from a single-cooling event. Road Materials and Pavement Design, 14(sup1), 201-211.
6. Glover, C. J., Martin, A. E., Chowdhury, A., Han, R., Prapaitrakul, N., Jin, X., & Lawrence, J. (2009). Evaluation of binder aging and its influence in aging of hot mix asphalt concrete: literature review and experimental design (No. FHWA/TX-08/0-6009-1).
7. Ahmed, Z., Marukic, I., Zaghloul, S., & Vitillo, N. (2005). Validation of enhanced integrated climatic model predictions with New Jersey seasonal monitoring data.

Transportation Research Record: Journal of the Transportation Research Board, (1913), 148-161.

8. Lytton, R. L., Uzan, J., Fernando, E. G., Roque, R., Hiltunen, D., & Stoffels, S. M. (1993). Development and validation of performance prediction models and specifications for asphalt binders and paving mixes (Vol. 357). Washington, DC: Strategic Highway Research Program.
9. Luo, X., Gu, F., & Lytton, R. L. (2016). Kinetics-based aging prediction of asphalt mixtures using field deflection data. Under review.
10. Luo, X., Gu, F., & Lytton, R. L. (2015). Prediction of Field Aging Gradient in Asphalt Pavements. Transportation Research Record: Journal of the Transportation Research Board, (2507), 19-28.
11. Lytton, R. L., Pufahl, D. E., Michalak, C. H., Liang, H. S., & Dempsey, B. J. (1993). An integrated model of the climatic effects on pavements. Report, FHWA-RD-90-033, Texas Transportation Institute, College Station, TX.
12. Brockwell, P. J., & Davis, R. A. (2006). Introduction to time series and forecasting. Springer Science & Business Media.
13. Soules, T. F., Busbey, R. F., Rekhson, S. M., Markovsky, A., & BURKE, M. A. (1987). Finite-Element Calculation of Stresses in Glass Parts Undergoing Viscous Relaxation. Journal of the American Ceramic Society, 70(2), 90-95.
14. Anderson, T. L. (2005). Fracture mechanics: fundamentals and applications. CRC press.

15. Zhang, Y., Luo, X., Luo, R., & Lytton, R. L. (2014). Crack initiation in asphalt mixtures under external compressive loads. Construction and Building Materials, 72, 94-103.

16. Han, R., Jin, X., & Glover, C. J. (2011). Modeling pavement temperature for use in binder oxidation models and pavement performance prediction. Journal of Materials in Civil Engineering, 23(4), 351-359.

17. Roque, R., Zou, J., Kim, Y. R., Baek, C., Thirunavukkarasu, S., Underwood, B. S., & Guddati, M. N. (2010). Top-down cracking of hot-mix asphalt layers: Models for initiation and propagation. Transportation Research Board of the National Academies.

18. Myers, L. A., & Roque, R. (2002). Top-down crack propagation in bituminous pavements and implications for pavement management. Journal of the Association of Asphalt Paving Technologists, 71.

19. Zhang, Z., Roque, R., & Birgisson, B. (2001). Evaluation of laboratory-measured crack growth rate for asphalt mixtures. Transportation Research Record: Journal of the Transportation Research Board, (1767), 67-75.

20. Roque, R., Sankar, B., & Technologists, A. P. (1999). Determination of Crack Growth Rate Parameters Of Asphalt Mixtures Using the Superpave lOT.

21. Bari, J., & Witczak, M. (2006). Development of a new revised version of the Witczak E* predictive model for hot mix asphalt mixtures (with discussion). Journal of the Association of Asphalt Paving Technologists, 75.

22. Witczak, M. W., & Sullivan, B. (2001). Superpave support and performance models management. Simple Performance Test: Test Results and Recommendations. NCHRP, 9-19.

23. Harmelink, D., & Aschenbrener, T. (2003). Extent of top-down cracking in Colorado (No. CDOT-DTD-R-2003-7).